Growth of ferroelectric $Ba_{0.8}Sr_{0.2}TiO_3$ epitaxial films by UV pulsed laser irradiation of chemical solution derived precursor layers

A. Queraltó[1], A. Pérez del Pino*[,1], M. de la Mata[1], J. Arbiol[1,2], M. Tristany[1], A. Gómez[1], X. Obradors[1], T. Puig[1]

[1]Institut de Ciència de Materials de Barcelona, Consejo Superior de Investigaciones Científicas (ICMAB-CSIC), Campus UAB, 08193 Bellaterra, Catalonia, Spain.

[2]Institució Catalana de Recerca i Estudis Avançats (ICREA), Passeig Lluís Companys, 23, 08010 Barcelona, Catalonia, Spain

***** Corresponding Author

Tel. +34 935801853

E-mail: aperez@icmab.es

Abstract

Highly crystalline epitaxial $Ba_{0.8}Sr_{0.2}TiO_3$ (BST) thin-films are grown on (001)-oriented $LaNiO_3$-buffered $LaAlO_3$ (LNO/LAO) substrates by pulsed laser irradiation of solution derived barium-zirconium-titanium precursor layers using a UV Nd:YAG laser source at atmospheric conditions. The structural analyses of the obtained films, studied by X-ray diffractometry and transmission electron microscopy, demonstrate that laser processing allows the growth of tens of nm-thick BST epitaxial films with crystalline structure similar to that of films obtained through conventional thermal annealing methods. However, the fast pulsed nature of the laser employed leads to crystallization kinetic evolution orders of magnitude faster than in thermal treatments. The combination of specific photothermal and photochemical mechanisms are the main responsible for the ultrafast epitaxial laser-induced crystallization. Piezoresponse microscopy measurements demonstrate equivalent ferroelectric behavior in laser and thermally annealed films, being the piezoelectric constant ~25 pm V^{-1}.

Text

Barium strontium titanate (BST) with Sr stoichiometry lower than 0.3 is a lead-free ferroelectric material which dielectric permittivity can be significantly tuned via an applied dc electric field. BST in thin film assembly shows great promise for the fabrication of devices such as tunable RF and microwave components, nonvolatile random access memories and microelectromechanical systems (MEMS).[1-3] Additionally, they offer the advantages of low voltage tunability and high speed cycling as compared to other materials.[4] In most cases, BST films have a polycrystalline microstructure that degrades its ferroelectric properties causing functional problems. Thus the fabrication of highly crystalline and epitaxial BST films through low cost and high integrability methods represents a major challenge.

In this sense, chemical solution deposition (CSD) techniques are able to achieve a controlled growth of functional highly-crystalline epitaxial oxide thin films and nanostructures through versatile and low-cost routes.[5-8] However, these techniques require of high temperature heat treatments of previously pyrolyzed metal organic precursor layers for obtaining the crystallization of the oxide films. Inconveniences of conventional annealing treatments are the time-consuming processing and the unfeasibility to easily achieve a spatially-resolved crystallization of materials in a simple way. Thus, laser processing appears as an outstanding alternative since it exhibits a significantly fast and localized thermal effect which could overcome thermal annealing limitations for example in the production of patterned micro- and nanostructures or in the growth of films on temperature sensitive substrates. It is well known that laser radiation can provoke very rapid photochemical - photothermal mechanisms in surface materials which can totally transform their crystalline structure.[9] Recently, direct nucleation and growth of epitaxial VO_2, $Ce_{0.9}Zr_{0.1}O_{2-y}$, Sb-doped SnO_2 and perovskite manganites (LMO, LSMO) thin films by laser irradiation of CSD precursors has been demonstrated.[10-15] Besides, the UV light-induced growth of polycrystalline ferroelectric oxides films such as BST has been already reported.[16-20] In this letter, we present our studies on laser-induced epitaxial growth of $Ba_{0.8}Sr_{0.2}TiO_3$ nanometric thin films deposited on (001)-oriented $LaNiO_3/LaAlO_3$ (LNO/LAO) substrates. The progress of films' crystalline status with the effective treatment time is

investigated. Moreover, the comparison of structural and functional properties of laser processed and thermally annealed samples is presented.

For the samples preparation, thoroughly cleaned (001)-oriented LAO single crystal (Crystec Gmbh) substrates of 5×5 mm^2 were coated with CSD-derived (001)$LaNiO_3$ epitaxial layers annealed at 700ºC, 10ºC min^{-1} for 1h in oxygen. The synthesis of LNO solutions with a 0.2M concentration in La consisted of dissolving lanthanum (III) nitrate and nickel (II) acetate salts (Sigma-Aldrich) in 2-methoxyethanol and refluxing at 125ºC for several hours. Deposition on LAO was performed using spin-coating (6000 rpm for 2 min). Single crystal substrates were 0.5 mm-thick, while LNO buffer layers had a thickness of ~25 nm. These LNO layers presented a high metallic behavior equivalent to that of films produced by physical techniques. Precursor solutions of BST with a 0.3M concentration in Ti were synthesized from barium (II) and strontium (II) acetate salts (Sigma-Aldrich) diluted in propionic acid and stirred for 3h at room temperature. Then, titanium (IV) isopropoxide was added to the mix, stabilized with acetylacetone. A small volume of solution (14 μL) was spin-coated (same conditions reported for LNO) on buffered LAO substrates. After deposition, the metal-organic Ba-Sr-Ti precursor film was pyrolyzed with conventional thermal treatments at 450ºC for 10 min to fully decompose the organic compounds and an amorphous film of about 40 nm was obtained. Laser irradiation of pyrolyzed precursor layers was performed with a Nd:YAG laser system (Brilliant, Quantel) emitting pulses of 266 nm wavelength with 3 ns in duration at a repetition rate of 10 Hz. The laser beam of 6 mm in diameter had a nearly Gaussian spatial distribution. Then, the samples were irradiated with a fixed number of accumulated pulses at 1 mm regularly spaced locations, leading to 80% of beam overlapping, in order to minimize non-uniform crystallization effects. Irradiation of films was accomplished in air with a substrate temperature of 400ºC for obtaining enhanced crystallinity of BST films. The laser fluence (measured at the maximum of the Gaussian beam) used in this work for crystallization of the amorphous BST films was set to 40 mJ cm^{-2}.

Amorphous pyrolyzed BST precursor films can be considered to contain mainly Ba-O, Sr-O and Ti-O bonds, as well as unsaturated bonds. Reported Ba-O, Sr-O and Ti-O bond dissociation energies are 563 kJ mol^{-1} (5.9 eV/bond), 454 kJ mol^{-1} (4.7 eV/bond) and 662 kJ mol^{-1} (6.9 eV/bond), respectively.[21] The values associated to Ba-O and Ti-O bonds are larger than the 4.7 eV photon energy of the laser radiation employed.

However, the Sr-O bond dissociation energy is comparable to that value. Consequently, laser irradiation of Sr-O bonds might provoke their direct chemical decomposition and light-driven reactivity (photoelectronic / photochemical mechanisms). Since Sr element concentration is relatively low in the material, we can consider the main fundamental mechanisms between laser light and film-matter being thermally activated (photothermal) for first approximation calculations. Nevertheless, it should be taken into account that the laser-induced thermal effects and corresponding physico-chemical mechanisms will be more prominent than those predicted from just photothermal estimation due to photoelectronic processes. Laser-induced photothermal mechanisms were simulated solving the heat equation by means of finite elements using COMSOL 4.4 Multiphysics software.[10] Additional information is included in Supplemental Material.[22] The optical and thermal properties of films' and substrates' materials were used in the calculations. Transmission and reflectance spectra of the BST amorphous films were acquired in the 200 – 750 nm range with a Varian Cary 5000 double-beam UV-Vis-NIR spectrophotometer (Figure S1)[22]. From these data, the refractive index (n) and extinction coefficient (κ) were extracted by the application of Denton's numerical model.[23] Hence, the absorption coefficient ($\alpha = 4\pi\kappa\lambda^{-1}$) and penetration depth (α^{-1}) were also calculated as a function of radiation wavelength (λ). The optical and thermophysical properties of films' and substrates' materials were estimated from Refs 24-29 and are summarized in Table S1.[22] The calculated penetration depth in both amorphous BST and epitaxial LNO films is about 48 nm, value which is larger than the films' thickness. Thus, around 57% of the incoming laser intensity is absorbed in pyrolyzed BST films, 41% of the transmitted radiation is absorbed in LNO buffer layers, and the remainder (about 26% of the total incident radiation) is transmitted and absorbed in the LAO substrate. Since part of the radiation arrives to LNO/LAO, additional photoelectronic processes could also appear due to their corresponding bond dissociation energies (Ni-O: 392 kJ mol^{-1} = 4.1 eV/bond; La-O: 799 kJ mol^{-1}= 8.3 eV/bond; Al-O: 512 kJ mol^{-1}= 5.3 eV/bond).[21] Photothermal simulations indicate that thermal pulses of hundreds of ns in duration are generated in BST films by the action of the laser pulses (Figure 1). The resulting heating-cooling rates can achieve about 10^{11} K s^{-1} inside the material, being the cooling time orders of magnitude longer than the heating one. After a 40 mJ cm^{-2} laser pulse absorption, the BST films' surface and interface can develop, respectively, maximum temperatures up to ~1200ºC and ~980ºC

leading to temperature gradients over 10^9 ºC m^{-1} during nanosecond time intervals across the BST layer. Notice that, melting temperatures of BST and LNO are not overpassed. Nonetheless, these temperatures would be underestimated if photochemical mechanisms were relevant in the process. We have assumed 600ºC as the minimum temperature in which ionic mobility can be large enough for the nucleation and growth of highly crystalline and epitaxial BST.[30] Accordingly, the calculated effective heating time of one laser pulse of 40 mJ cm^{-2} in which the temperature is larger than 600ºC is ~19 ns.

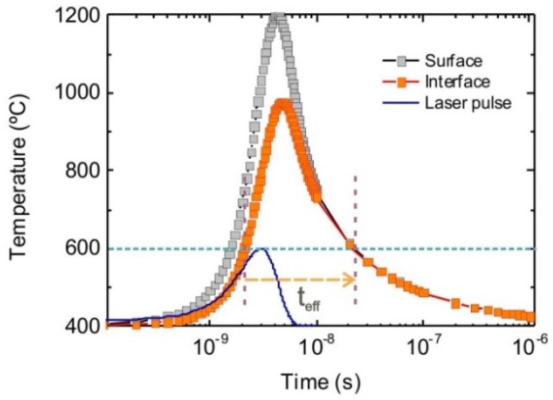

FIG. 1. Simulated temporal evolution of the temperature in BST film surface and BST/LNO interface when irradiated with a 40 mJ cm^{-2} laser fluence pulse.

Pyrolyzed BST precursor layers deposited on LNO/LAO were treated by accumulating between 2500 and 20000 laser pulses per site. In order to evaluate the crystalline evolution of the samples, X-ray diffraction (XRD) characterizations were accomplished using a Rigaku Rotaflex RU-200BV diffractometer with Cu-Kα radiation source (λ = 0.154 nm). Figure 2a shows the XRD diffractograms of samples processed by the accumulation of 2500, 10000 and 20000 pulses per site, as well as a non-irradiated sample. The diffractogram of the latter sample displays the LAO (002) peak located at ~48.2º and its weak k_β signal at ~43.1º, as well as the LNO (002) reflection at ~47.3º which is partially overlapped with the LAO (002) peak. The diffractograms of the irradiated samples exhibit, in addition, an intense BST (002) reflection located at ~45.9º. No additional polycrystalline reflections are recorded and the accumulation of laser pulses produces an increase of epitaxial BST peak intensity. We can state that laser

irradiation of pyrolyzed BST films produces the epitaxial growth of the final oxide phase from the initial amorphous material. A more detailed analysis by means of 2D-XRD using a GADDS system from Bruker, equipped with a 2-dimensional detector (λ = 0.154 nm), reveals heterogeneous nucleation of BST at the interface with LNO, in addition to homogeneous nucleation in other regions of the film (incomplete ring in the inset of Figure 2b). We can quantify the amount of epitaxial-to-polycrystalline BST present in the laser processed films by analyzing the corresponding 2D-XRD data as indicated in Ref. 31. As observed in Figure 2b, the epitaxial BST thickness, calculated as a function of the effective heating time of the overall laser treatment by multiplying the total number of accumulated pulses per zone and the effective heating time of one laser pulse (the effect of laser spot overlapping is also considered), rapidly increases with the effective heating time, reaching the full film thickness after just 2.4 ms. This evidences that further laser irradiation of the homogeneously nucleated polycrystalline material leads to a transformation into epitaxial grains which is driven by a reduction of the high surface energy of the polycrystalline grains (grain boundary energy).[10] The BST epitaxial growth rate, evaluated from the variation of epitaxial thickness with effective time, reaches values as high as 10^5 nm s^{-1}. Equivalent samples, heat treated by means of rapid thermal annealing (at 900ºC during 60-1800 s in oxygen flow, 20 ºC s^{-1} heating rate) were also produced for comparison. These samples also show epitaxial growth although the growth rate is considerably slower, ~0.1 nm s^{-1}, and full epitaxial film growth is obtained after ~600 s. Laser-induced specific photothermal mechanisms, mainly due to the development of huge temperature gradients, as well as photochemical mechanisms (reactivity enhancement of optically active chemical bonds) would cause the observed significantly faster epitaxial growth of BST in laser treated samples in comparison to thermally annealed ones.[9,10]

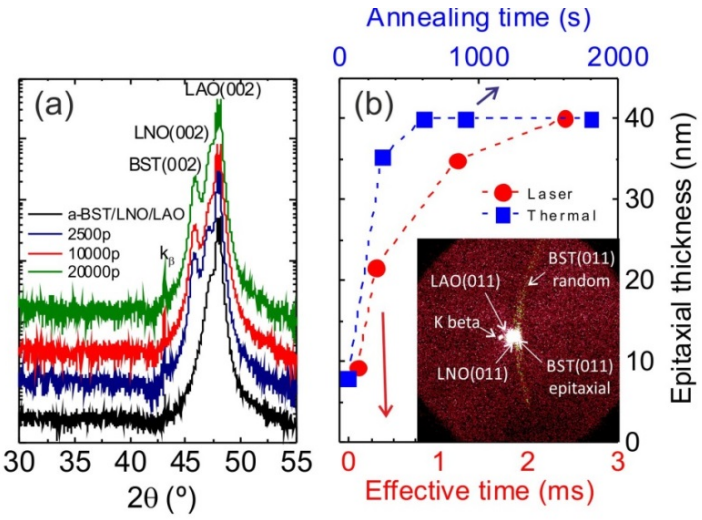

FIG. 2. (a) XRD diffractograms of a pyrolyzed film as well as the samples irradiated with different number of accumulated pulses (b) Calculated BST epitaxial thickness of samples obtained by laser treatment and rapid thermal annealing. Inset: 2D-XRD image centered at LAO (011) Bragg reflections for the quantification of the epitaxial crystals' fraction of the sample irradiated with 40 mJ cm^{-2} laser fluence and 2500 accumulated pulses.

High resolution transmission electron microscopy (HRTEM) analyses were carried out to study the crystalline quality of the obtained BST layers grown by laser processing. Cross-sectional TEM specimens were prepared by mechanical polishing and a final step of ion milling. HRTEM observations were carried out by means of a FEI Tecnai F20 microscope with a field-emission gun operated at 200 kV achieving a lateral resolution of 0.14 nm. Figure 3 shows a cross section of a laser irradiated sample with 20000 pulses/site (2.4 ms effective heating time) exhibiting a highly crystalline epitaxial heterostructure oriented with the LAO substrate along the [001] direction. We did not detect misfit dislocations at the LNO/LAO interface indicating a fully strained heteroepitaxy. This fact was checked by analyzing the power spectra which only shows one Bragg reflection set. The experimental LNO cell parameter is $a_{LNO,exp}$ = 3.788Å indicating a compression of the LNO layer of -1.6% driven by the substrate ($a_{LAO,bulk}$ = 3.788Å, $a_{LNO,bulk}$ = 3.850Å). The BST grown on the top of the LNO layer also shows an epitaxial structure oriented along the [001] direction. The measured lattice parameter of BST is $a_{BST,exp}$ = 3.884Å, which is compressed about -2.7% ($a_{BST,bulk}$ = 3.993Å). This

compression is induced by the LNO buffer layer, although in this case the film is partially strained with a remaining BST lattice parameter 2.5% larger than that of LNO (Figure 3).

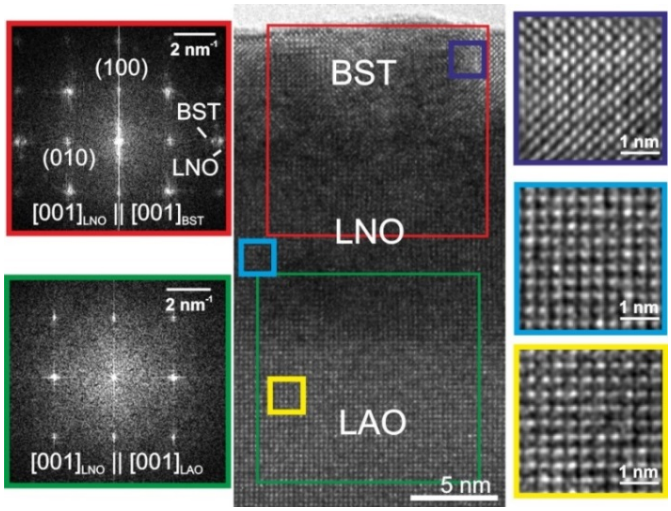

FIG. 3. TEM analysis of sample irradiated with 40 mJ cm^{-2} laser fluence and accumulating 20000 pulses/site. Frame colors indicate the corresponding studied zones.

Local ferroelectric performance of the samples was studied by piezoresponse force microscopy (PFM). The measurements were done using an Agilent 5500LS equipment in contact mode. Conductive diamond tips (AppNano) with a radius < 150 nm and a force constant between 0.1 - 0.6 N m^{-1} were used for the measurements. Typical analysis of writing experiments done in BST films irradiated by the accumulation of 10000 laser pulses/site (~1.2 ms of effective heating time, ~35 nm epitaxial thickness) and thermally annealed at 900ºC during 14400 s is shown in Figure 4a. Writing experiments were performed scanning 4×4 μm^2 squares poled with +7 V or -7 V bias, followed by 2×2 μm^2 squares scanned inward using inversed bias. Figure 4b reveals similar PFM amplitude-electric field loops for laser and thermally treated samples, though hysteretic behavior is slightly smaller in laser samples (additional loops are presented in Figure S2).[22] Phase hysteresis loops show well-saturated shapes, being the coercive field difference about 5.0-7.5×10^7 V m^{-1}. The effective piezoelectric constant d_{33}, calculated from the amplitude - phase loops, is shown in the inset of Figure 4b. The d_{33} values of the laser and thermal treated samples are, respectively, ~22 pm V^{-1} and ~27 pm V^{-1} at remanence (~130 kHz resonance frequency, 2.5 V_{AC}). These values are

comparable to those previously obtained in $BaTiO_3$ thin films developed by CSD with furnace treatments[32] and higher than in epitaxial $Ba_{0.6}Sr_{0.4}TiO_3$ layers grown on MgO and LAO substrates.[33]

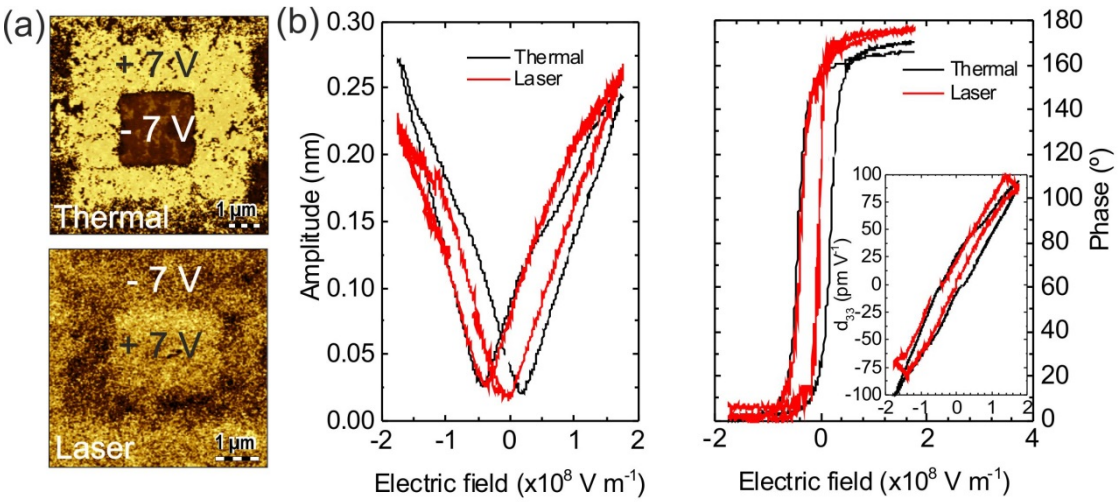

FIG. 4. PFM characterization of samples obtained by laser irradiation with 40 mJ cm^{-2} and 10000 accumulated pulses per site, and by thermal annealing at 900ºC during 14400 s. (a) switching phase images obtained by applying ±7 V, (b) amplitude-electric field butterfly and phase-electric field hysteresis loops. Inset: d_{33} constant as a function of electric field.

In summary, we have demonstrated the ability of UV laser irradiation technique combined with chemical solution deposition for fabricating tens of nanometers thick highly crystalline epitaxial BST/LNO/LAO films in a fast way. The obtained films exhibit ferroelectric switching with perpendicular polarization comparable to similar systems produced by time-consuming conventional annealing methods. The proposed fabrication method is cost-effective, it does not require vacuum technology, it allows the versatile production of patterns due to the local nature of laser irradiation, and it permits to considerably decrease the fabrication time.

This work was financed by the Ministry of Economy and Competitiveness under the projects MAT2011-28874-C02-01, ENE2014-56109-C3-3-R, MAT2014-51778-C2-1-R

and Consolider Nanoselect CSD2007-00041, by Generalitat de Catalunya (2009 SGR 770, 2014 SGR 753 and Xarmae) and by the Spanish National Research Council under the Contract No. 200960I015. AQ and MdlM are also grateful for JAE-Predoc fellowship and European Social Fund program. Fruitful discussions with Dr. Susagna Ricart for solution synthesis are also acknowledged.

References

[1] A. Tombak, J. P. Maria, F. Ayguavives, Z. Jin, G. T. Stauf, A. I. Kingon, and A. Mortazawi. IEEE Microw Wirel CO **12**, 3 (2002)

[2] R. Balachandran, B.H.Ong, H.Y.Wong, K.B.Tan and M.M. Rasat. Int. J. Electrochem. Sci. **7**, 11895 (2012)

[3] K. Entesari and G. M. Rebeiz. Int J RF Microw C E **18**, 86 (2008)

[4] H. Khassaf, N. Khakpash, F. Sun, N. M. Sbrockey, G. S. Tompa, T. S. Kalkur and S. P. Alpay. Appl. Phys. Lett. **104**, 202902 (2014)

[5] R. Schwartz, T. Schneller and R. Waser. C R Chimie **7**, 433 (2004)

[6] X. Obradors, F. Martínez-Julián, K. Zalamova, V.R. Vlad, A. Pomar, A. Palau, A. Llordés, H. Chen, M. Coll, S. Ricart, et al. Physica C **482**, 58 (2012)

[7] X. Obradors, T. Puig, S. Ricart, M. Coll, J. Gazquez, A. Palau, X. Granados. Supercond. Sci. Technol. **25**, 123001 (2012)

[8] S. Hoffmann and R.Waser. J.Eur.Ceram.Soc. **19**, 1339 (1999)

[9] D. Bãuerle, Laser Processing and Chemistry, Springer, Berlin (2000)

[10] A. Queraltó, A. Pérez del Pino, M. de la Mata, J. Arbiol, X. Obradors and T. Puig. Cryst. Growth Des. **15**, 1957 (2015)

[11] M. Nishikawa, T. Nakajima, T. Kumagai, T. Okutani and T. Tsuchiya. Appl. Phys. A **100**, 297 (2010)

[12] T. Tsuchiya, T. Nakajima and K. Shinoda. Appl. Phys. B **113**, 333 (2013)

[13] T. Nakajima, T. Tsuchiya, M. Ichihara, H. Nagai and T. Kumagai. Chem. Mater. **20**, 7344 (2008)

[14] T. Tsuchiya, T. Nakajima and T. Kumagai. Appl. Surf. Sci. **255**, 9804 (2009)

[15] T. Nakajima, K. Shinoda and T. Tsuchiya. Chem. Soc. Rev. **43**, 2027 (2014)

[16] H.Imai, Ultraviolet (UV) irradiation. Sol-Gel science and technology, processing, characterization and applications. Vol. I, Ed. S.Saka. Kluwer Ac. Publ., Norwell (2004)

[17] S. S. N. Bharadwaja, T. Dechakupt, S. Trolier-McKinstry and H. Beratan. J. Am. Ceram. Soc. **91**, 1580 (2008)

[18] I. Bretos, R. Jimenez, A. Y. Wu, A. I. Kingon, P. M. Vilarinho and M. L. Calzada. Adv. Mater. **26**, 1405 (2014)

[19] O. Baldus, W. Krasser, S. Hoffmann, R. Waser and E. W. Kreutz. Integr. Ferroelectr. **30**, 129 (2000)

[20] O. Baldus and R. Waser. Appl. Phys. A. **80**, 1553 (2005)

[21] J. A. Dean, Lange's handbook of chemistry, 15th ed., McGraw-Hill, New York (1999)

[22] See supplemental materials at [XXX] for the supplementary figures of measured optical properties of amorphous BST films, the optical and thermophysical parameters of BST, LNO and LAO materials used in the photothermal simulations and additional

PFM measurements. A brief explanation of the photothermal simulations is also included in the supplemental materials.

[23] R. E. Denton, J. Phys. D **5**, 852 (1972)

[24] Mistrik, J., T. Yamaguchi, D. Franta, I. Ohlidal, G. J. Hu and N. Dai. Appl Surf Sci **244**, 431 (2005)

[25] Lai, S. C., H. T. Lue, K. Y. Hsieh, S. L. Lung, R. Liu, T. B. Wu, P. P. Donohue and P. Rumsby. J Appl Phys **96**, 2779 (2004)

[26] Zinkevich, M. and F. Aldinger. J Alloy Compd **375**, 147 (2004)

[27] Zeng, X., L. Zhang, G. Zhao, J. Xu, Y. Hang, H. Pang, M. Jie, C. Yan and X. He. J Cryst Growth **271**, 319 (2004)

[28] Michael, P. C., J. U. Trefny and B. Yarar. J of Appl Phys **72**, 107 (1992)

[29] Davitadze, S. T., S. N. Kravchun, B. A. Strukov, B. M. Goltzman, V. V. Lemanov and S. G. Shulman. Appl Phys Lett **80**, 1631 (2002)

[30] U. Hasenkox, S. Hoffmann and R. Waser, J. Sol-Gel Sci. Techn. **12**, 67 (1998)

[31] A. Llordés, A. Palau, J. Gázquez, M. Coll, R. Vlad, A. Pomar, J. Arbiol, R. Guzmán, S. Ye, V. Rouco, et al. Nat. Mat. **11**, 329 (2012)

[32] Y. Guo, K. Suzuki, K. Nishizawa, T. Miki and K. Kato. J Cryst Growth **284**, 190 (2005)

[33] H. X. Cao and Z. Y. Li. Phys Lett A **334**, 429 (2005)